Adaptive piezoelectric metamaterials leveraging non-uniform local resonators

Ting Wang, Joshua Dupont, J. Tang
Department of Mechanical Engineering
University of Connecticut
Storrs, CT 06269, USA

ABSTRACT

Metamaterials with locally resonant unit cells based on piezoelectric shunting have led to a new way of realizing elastic/acoustic wave manipulation with online tuning capability. One limitation of uniform locally resonant metamaterials with identical unit cells is their relatively narrow bandgap. Recently, the concept of graded metamaterials with non-uniform local resonators has emerged as a promising approach for improvement. In this research, we explore an adaptive piezoelectric metamaterial-based metamaterial design with spatially varying piezoelectric shunt circuits integrated with negative capacitance. Through systematic parametric analysis, a new design is identified to take advantage of the graded resonant shunt to enhance wave manipulation performance and enlarge the bandgap. Case investigations are presented to demonstrate the feasibility.

Keywords: graded piezoelectric metamaterial, wave attenuation, shunt circuit, bandgap, negative capacitance

1. INTRODUCTION

Metamaterials are a unique artificial composite with periodic arrangement of unit cells capable of generating bandgap behavior in which waves cannot propagate. Wave manipulation has also been explored to realize wave focusing [1], wave filtering [2] and wave isolation [3]. It is well-known that there are two kinds of mechanisms to produce frequency bandgaps, i.e., Bragg scattering and local resonance. The Bragg scattering usually occurs in the high frequency region as it is highly dependent on the size of the unit cell [4]. The local resonance mechanism, on the other hand, can be synthesized within the sub-wavelength regime [5]. An interesting research subject is to widen the bandgap of locally resonant metamaterials. Various mechanical designs of local resonators are proposed to create and widen the bandgap, through the usage of structures such as origamis [6], membranes and rings [7], and multi-degree-of-freedom local resonators [8]. The piezoelectric metamaterials using inductive shunting together with the piezoelectric inherent capacitance, i.e., the LC resonance, have received much attention as the inductance element can potentially be online tuned, yielding adaptive manipulation of waves. In order to broaden the bandgap, several circuitry integration schemes have been proposed, including negative capacitance (NC) circuit [9, 10], nonlinear local resonator [11], and switching circuit [12].

These investigations, however, primarily focus on metamaterial designs with periodically arranged arrays of identical local resonators. More recently, the concept of graded metamaterials where material or geometric properties of the unit cells are allowed to vary slightly has been explored, aiming at enhanced wave attenuation performance [13-18]. For example, with spatially varying LC resonant frequencies, multiple LC resonant bandgaps can be created within the bandgap region, forming an overall enlarged bandgap. The gradient resonant frequencies can be realized in piezoelectric shunts by varying inductance [13, 15], varying electrode length [13], and varying the equivalent capacitance by adding NC elements [16, 18]. While the bandgap can be widened, there are many resonant peaks inside the bandgap region which require load resistance to smooth through damping. On the other hand, the continuous attenuation region after smoothing with resistance may become a pseudo bandgap with poor attenuation characteristics. Relatively few papers offer solutions to this issue, with exceptions including some optimization analyses [13, 17].

It is worth noting that the integration of NC has attracted increasing attention in recent years due to significantly improved vibration control performance [19, 20]. In metamaterial synthesis, it has been investigated that NC has promising potential in broadening single bandgap in conventional uniform piezoelectric metamaterials [10]. Additionally, it is found that NC is capable of combining neighboring Bragg scattering bandgap and local resonance bandgap to form broad and low-frequency bandgaps [9]. This gives rise to the new idea of graded piezoelectric metamaterials with non-

uniform LC resonant shunt circuits integrated with NC for enhanced broadband wave attenuation performance. The objective of this research is to explore the feasibility of using NC to further widen the bandgap and address the weak attenuation of recently proposed graded metamaterials. Section 2 provides the analytical modeling of graded metamaterials using the transformation method. In Section 3, we present the design strategy of the proposed NC integrated graded metamaterials. In Section 4, the effect of NC to the wave attenuation performance of graded metamaterials is analyzed under different load resistance and frequency spacing. Section 5 concludes this report.

2. MODELING OF GRADED PIEZOELECTRIC METAMATERIAL BEAM

We considering a piezoelectric metamaterial beam as shown in Figure 1, where the transducers are periodically attached to the host beam in a unimorph configuration. For each unit cell, the piezoelectric transducer acts electrically as a capacitor, which then is shunted with an inductor to form LC local resonance. In the present study, the graded piezoelectric metamaterial is formed by non-uniform unit cells connected to different local resonant circuits to produce gradient LC resonance frequency, as illustrated in Figure 1(a). A resistor is integrated into each unit cell circuit. In this research, an additional NC is integrated with LC resonant circuit to improve the wave attenuation performance of graded metamaterial beam even further. The negative impedance converter, shown in Figure 1(b), is utilized to realize NC.

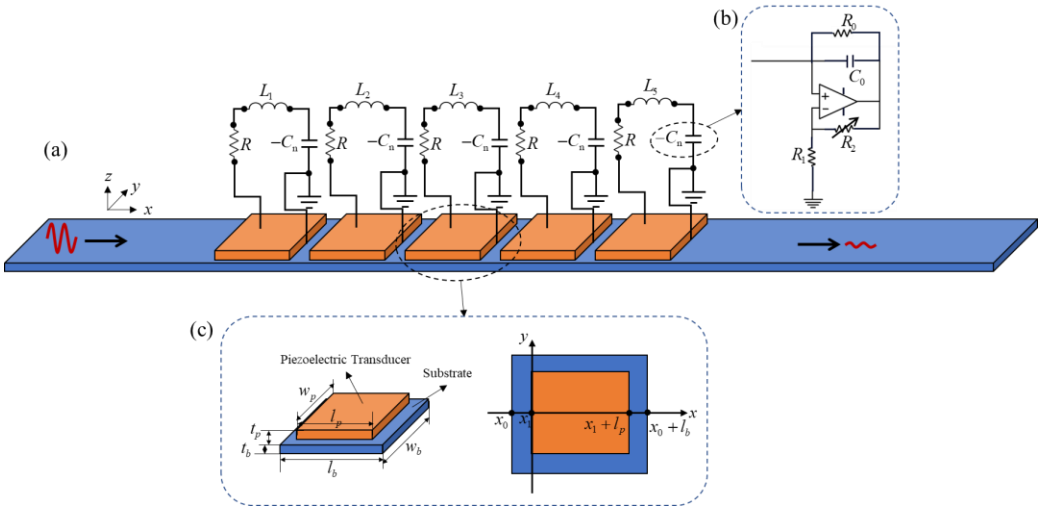

Figure 1. Schematic of (a) the graded piezoelectric metamaterial beam with non-uniform local LC resonant unit integrated with NC, (b) NC circuit, (c) close-up view of a unit cell.

To establish the analytical model, the transfer matrix method is employed to compute the transmission ratio responses of the entire piezoelectric metamaterial beam [5, 14]. By associating adjacent unit cells through continuity conditions, the dynamic transformation matrices of all unit cells can be assembled. When the harmonic incident wave propagates through one unit cell as shown in the top view of Figure 1, the wave actually propagates through 2 types of segments, i.e., the segments without piezoelectric transducer from x_0 to x_1 and from x_1+l_p to x_0+l_b, and the segment with piezoelectric transducer from x_1 to x_1+l_p. Based on the Timoshenko beam theory [5] and 1D constitutive relation of piezoelectric transducer under 31-mode coupling, the dynamic states matrices for the beam segment with and without the piezoelectric transducer can be written as,

$$\mathbf{Y_p}=\begin{bmatrix} w & \theta & M & R \end{bmatrix}^T=\mathbf{B_p}\mathbf{V_p}=\mathbf{B_p}\begin{bmatrix} \bar{A}_1 e^{\lambda_1 x} & \bar{A}_2 e^{\lambda_2 x} & \bar{A}_3 e^{\lambda_3 x} & \bar{A}_4 e^{\lambda_4 x} \end{bmatrix}^T \tag{1}$$

$$\mathbf{Y_b}=\begin{bmatrix} w^b & \theta^b & M^b & R^b \end{bmatrix}^T=\mathbf{B_b}\mathbf{V_b}=\mathbf{B_b}\begin{bmatrix} \bar{A}_1 e^{\lambda_1^b x} & \bar{A}_2 e^{\lambda_2^b x} & \bar{A}_3 e^{\lambda_3^b x} & \bar{A}_4 e^{\lambda_4^b x} \end{bmatrix}^T \tag{2}$$

where w and θ are the assumed harmonic solutions of vertical displacement and rotating angle, respectively. M and R are the bending moment and shear force. The general wave solution of vertical displacement w can be expressed as the linear combination of all four propagating eigenmodes $w=\sum_{n=1}^{4}\bar{A}_n e^{\lambda_n x}$, each elements in matrix $\mathbf{V}$ representing one

propagating eigenmodes under one eigenvalue λ and its corresponding undetermined constant amplitude component $\bar{A}$. The subscript and superscript p and b represent the segments with and without the piezoelectric transducer, respectively. The matrix $\mathbf{B}$ represents the transformation matrix. The dynamic states for the two ends of the three aforementioned segments can be obtained as,

$$x = x_0 \rightarrow x_1 : \mathbf{Y_b}(x_1) = \mathbf{B_b}\mathbf{D_{b1}}\mathbf{B_b^{-1}}\mathbf{Y_b}(x_0) \tag{3}$$

$$x = x_1 \rightarrow x_1 + l_p : \mathbf{Y}_p(x_1 + l_p) = \mathbf{B_p}(x_1 + l_p)\mathbf{D_p}\mathbf{B_p^{-1}}(x_1)\mathbf{Y_b}(x_1) \tag{4}$$

$$x = x_1 + l_p \rightarrow x_0 + l_b : \mathbf{Y_b}(x_0 + l_b) = \mathbf{B_b}\mathbf{D_{b2}}\mathbf{B_b^{-1}}\mathbf{Y_b}(x_1 + l_p) \tag{5}$$

where $\mathbf{D_{b1}}$ and $\mathbf{D_{b2}}$ are diagonal matrices in terms of the eigenvalue λ and dimensional parameters. The transformation matrix $\mathbf{B_b}$ of segment without the piezoelectric transducer is independent of current location x, while the transformation matrix $\mathbf{B_p}$ of segment with the piezoelectric transducer is dependent on current location x and electrical impedance Z_{sh}. Finally, combing Equations (3), (4) and (5), the transformation of dynamic states at two ends of the whole unit cell can be obtained as,

$$x = x_0 \rightarrow x_0 + l_b : \mathbf{Y_b}(x_0 + l_b) = \mathbf{T_{pb1}}\mathbf{Y_b}(x_0) \tag{6}$$

where $\mathbf{T_{pb1}}$ is the transformation matrix of dynamic states, which can be used to obtain dispersion relation. After we substitute Equations (1) and (2) into equation (6), the transformation of propagating wave can be expressed as,

$$x = x_0 \rightarrow x_0 + l_b : \mathbf{V_b}(x_0 + l_b) = \mathbf{T_{pb2}}\mathbf{V_b}(x_0) \tag{7}$$

$$\mathbf{T_{pb2}} = \mathbf{D_{b2}}\mathbf{B_b^{-1}}\mathbf{B_p}(x_1 + l_p)\mathbf{D_p}\mathbf{B_p^{-1}}(x_1)\mathbf{B_b}\mathbf{D_{b1}}\mathbf{B_b^{-1}}\mathbf{B_b} \tag{8}$$

where $\mathbf{T_{pb2}}$ is the transformation matrix from incident wave to outgoing wave, which can be utilized to compute the transmission ratio.

The overall transformation matrix of propagating wave is modeled by assembling the transformation matrices of all N unit cells. A uniform piezoelectric metamaterial beam has identical unit cells constructed with identical LC circuits, resulting in N identical transformation matrices corresponding to N identical unit cells. Hence, the overall transformation matrix of propagating wave of uniform metamaterial beam can be expressed as,

$$\mathbf{T_{pb2}^{all}} = (\mathbf{T_{pb2}})^N \tag{9}$$

In this research, the unit cell is shunted with spatially varying inductive circuits to generate graded LC resonant frequencies. The spatially varying circuit impedance of the i^{th} unit cell can be written as,

$$Z_{sh}^i = R + i\omega L_i \tag{10}$$

where R is the identical resistance value that each unit cell is integrated with, ω is the frequency, and L_i is the inductance value in the i^{th} unit cell shunt circuit. Then, the corresponding LC resonant frequency of the i^{th} unit cell is

$$f_{L_i} = \frac{1}{2\pi\sqrt{C_p L_i}} \tag{11}$$

where C_p is the inherent capacitance of the piezoelectric transducer.

Note that the transformation matrix $\mathbf{B_p}$ of segment with piezoelectric transducer for a single unit cell is related to circuit impedance. It means that the i^{th} non-uniform unit cell with different Z_{sh}^i has different $\mathbf{B_p}$, yielding different $\mathbf{T_{pb2}}$. Therefore, the overall transformation matrix of propagating wave of non-uniform metamaterial beam can be obtained as,

$$\mathbf{T}_{\mathbf{pb2}}^{\mathbf{all}} = \prod_{i=1}^{N} \mathbf{T}_{\mathbf{pb2}}^{\mathbf{i}} = \prod_{i=1}^{N} \mathbf{D}_{\mathbf{b2}} \mathbf{B}_{\mathbf{b}}^{-1} \left(\mathbf{B}_{\mathbf{p}}^{\mathbf{i}} (x_1 + l_p) \right) \mathbf{D}_{\mathbf{p}} \left(\mathbf{B}_{\mathbf{p}}^{\mathbf{i}} (x_1) \right)^{-1} \mathbf{B}_{\mathbf{b}} \mathbf{D}_{\mathbf{b1}} \mathbf{B}_{\mathbf{b}}^{-1} \mathbf{B}_{\mathbf{b}} \tag{12}$$

where $\mathbf{B}_{\mathbf{p}}^{\mathbf{i}}$ is the transformation matrix of the segment with piezoelectric transducer in the i^{th} non-uniform unit cell. $\mathbf{T}_{\mathbf{pb2}}^{\mathbf{i}}$ is the transformation matrix of propagating wave of the i^{th} non-uniform unit cell. The overall transmission ratio is defined as the ratio of the displacement of the transmitted wave to the displacement of the incident wave [14, 15, 17], given as,

$$\left| \mathrm{TR}(\omega) \right| = \left| \frac{\tilde{\mathbf{V}}_{\mathbf{b}}^{\mathbf{N}} (x_0 + l_b)}{\tilde{\mathbf{V}}_{\mathbf{b}}^{\mathbf{1}} (x_1)} \right| \tag{13}$$

where $\tilde{\mathbf{V}}_{\mathbf{b}}^{\mathbf{1}} (x_1)$ represents the displacement amplitude of incident wave at location x_1 of the first unit cell. $\tilde{\mathbf{V}}_{\mathbf{b}}^{\mathbf{N}} (x_0 + l_b)$ represents the displacement amplitude of transmitted wave at output location $x_0 + l_b$ of the last N^{th} non-uniform unit cell. $\tilde{\mathbf{V}}_{\mathbf{b}}^{\mathbf{1}} (x_1)$ and $\tilde{\mathbf{V}}_{\mathbf{b}}^{\mathbf{N}} (x_0 + l_b)$ can be obtained from the constant amplitude component $\bar{A}$ under each eigenvalue λ of matrix $\mathbf{V}$ in Equations (1) and (2).

3. DESIGN STRATEGY OF ADAPTIVE BROADBAND WAVE ATTENUATION

Our hypothesis here is that the enhanced electromechanical coupling effect of NC improves the broadband wave attenuation performance of graded piezoelectric metamaterials. Without loss of generality, in this research, we adopt five unit cells with spatially varying shunt circuits for demonstration. The inductance value is set to be graded, in order to facilitate graded LC resonant frequencies. The linear grading pattern [15] is employed to determine the non-uniform resonant frequency of each unit cell such that

$$f_{L_i} = f_t + 2\Delta f - 4\Delta f \left(\frac{i-1}{N-1} \right) \tag{14}$$

where f_t is the target frequency of the central unit cell ($N = 3$), which is set to be constant value 150Hz in this study. Δf represents the frequency spacing of adjacent unit cells. Without NC integration, by substituting the designed resonant frequency of each unit cell based on Equation (14) back to Equation (11), the required L_i values for non-uniform unit cells can be obtained.

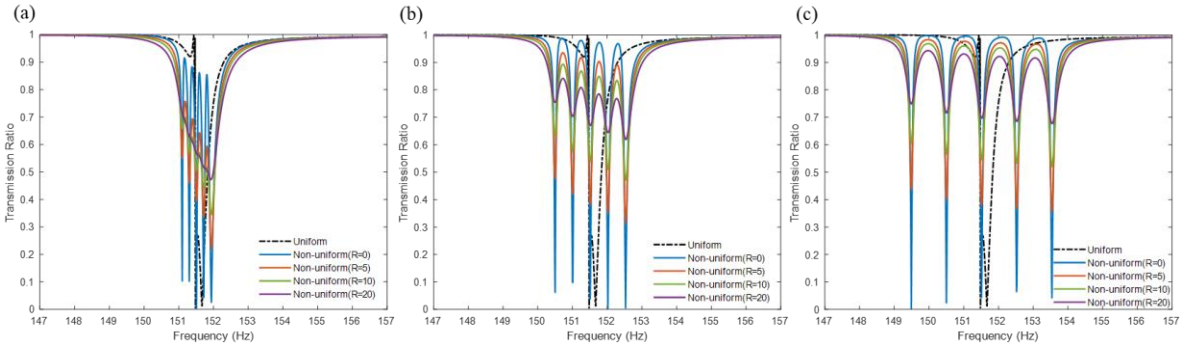

Figure 2. Transmission ratio responses of non-uniform metamaterials with different frequency spacings: (a) $\Delta f = 0.2\mathrm{Hz}$, (b) $\Delta f = 0.5\mathrm{Hz}$, (c) $\Delta f = 1\mathrm{Hz}$

Taking the conventional uniform piezoelectric metamaterial beam as a reference, Figure 2 plots the transmission ratio of the proposed graded beam with different frequency spacing Δf and R values. Compared to the uniform unit cell case which creates a single narrow bandgap near one local resonant frequency, the non-uniform metamaterial beam generates multiple scattered resonant peaks inside the attenuation region. The fundamental idea behind the graded piezoelectric metamaterial beam is to overlap those multiple bandgap regions to form a wider "aggregated" bandgap. Therefore, the

frequency spacing Δf is of significant importance in aggregating those scattered bandgap regions. The small frequency spacing in Figure 2(a) yields a wider overall bandgap region as compared to the unsuccessful aggregation with the completely separated adjacent bandgaps in Figure 2(c) under larger frequency spacing. In addition, as previous studies have indicated, using load resistor R can suppress those sharp local resonant peaks to achieve a continuous attenuation region [17, 18]. However, the smoothed bandgap by adequately tuning the load resistance R results in a pseudo bandgap where the transmission ratio becomes large, i.e., at around -10dB (around 0.3) for wave attenuation [13, 14, 18]. The transmission ratio becomes as large as 0.5 with $R = 20\Omega$ damping, as illustrated in Figure2(a). Reduced performance in the transmission ratio is observed with larger Δf as shown in Figures 2(b) and 2(c).

Building upon the previous studies, we propose to integrate additional NC circuits in series to the non-uniform LC resonant circuit to address the issue of pseudo bandgap. The parameter δ is utilized to represent the relative ratio of NC value C_n and the inherent piezoelectric capacitance C_p, i.e., $\delta = -C_n/C_p$. $|\delta| > 1$ is required for system stability. The closer $|\delta|$ is to 1, the larger the portion of C_p offset by C_n and the larger the electromechanical coupling of piezoelectric transducer [20]. The additional NC integration strategy has been envisioned as an ideal complement to bandgap control in conventional uniform piezoelectric metamaterial beam, e.g., broaden bandgap width and tunable bandgap location. As displayed in Figure 3, the NC integration leads to significant changes in bandgap width that a single narrow bandgap is widened directly, and with smaller $|\delta| = 1.1$, the bandgap width can be widened even more significantly. At the same time, the shifting bandgap location in Figure 3 illustrates the ability to tune the bandgap location by NC integration, i.e., the upper and lower frequency boundaries of bandgap are correlated to $|\delta|$ [14].

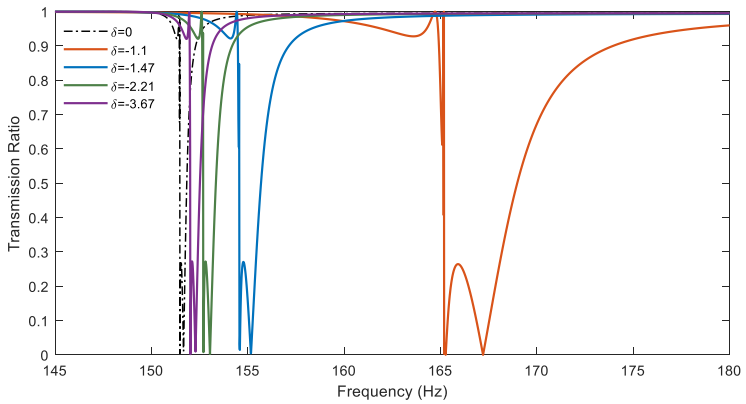

Figure 3. Transmission ratio responses of conventional uniform metamaterials with different δ values.

The well-known bandgap control ability of NC in conventional uniform piezoelectric metamaterial beam has motivated this analysis. In this research, NC integration is employed to non-uniform unit cells for enhanced bandgap control in graded metamaterial beam, while non-uniform inductive circuit is still utilized to produce non-uniform local resonances. With NC integrated with non-uniform LC resonant circuit as shown in Figure 1(a), the circuit impedance of each non-uniform unit cell changes from Equation (10) to the below expression,

$$Z_{sh}^{i} = R + i\omega L_i + \frac{1}{-i\omega C_n} \tag{15}$$

With the NC integration, the equivalent capacitance C_t in the shunt circuit changes accordingly. In order to guarantee the same gradient resonant frequency pattern f_{L_i} in equation (14), the required inductance value L_i' of each non-uniform unit cell will need to be changed such that

$$L_i' = \frac{1}{\left(2\pi f_{L_i}\right)^2 C_t} = \frac{1}{\left(2\pi f_{L_i}\right)^2 \dfrac{C_p C_n}{\left(C_n - C_p\right)}} \tag{16}$$

According to Equation (16), the NC integration also increases the equivalent capacitance C_t, leading to significantly reduced inductance value L_i', which may lead to advantage in practical circuit implementation.

4. CASE STUDIES

There are three design variables involved in the proposed non-uniform piezoelectric metamaterial beam, i.e., the NC ratio δ, the resistance value R, and frequency spacing Δf. In order to investigate the advantages of NC to the non-uniform metamaterial beam, the frequency spacing Δf is set to 0.2Hz, which is sufficiently small to ensure the overlapping of multiple resonant bandgaps. Under different δ cases, the transmission ratios with different R values are illustrated in Figure 4. It is observed that the benefits of NC integration in conventional uniform piezoelectric metamaterial beam also apply to graded beam case with non-uniform unit cell.

Specifically, compared to the graded beam design without NC integration ($\delta = 0$, $R = 0$), the NC integrated graded metamaterial beam ($\delta \neq 0$, $R = 0$) is capable of further expanding the aggregated bandgap width by up to 294%, reducing the amplitudes of multiple resonant peaks, and tuning the bandgap location. Similar to the results in Figure 3, the smaller $|\delta|$ yields even wider bandgap and larger bandgap location-shifting effects. It is demonstrated that by simply tuning δ, not only bandgap width, but also bandgap location (upper and lower frequency boundaries) can be tunable.

Meanwhile, the smoothing effect from R still applied to NC integration case. Moreover, the graded beam with NC integration requires smaller R value to achieve the same smoothing effect as graded beam without NC integration. As shown in Figure 4, $R = 10\Omega$ is not enough for graded beam without NC integration, since the smoothed curve is still wavy, while $R = 5\Omega$ is already enough for graded beam with NC integration to achieve smooth and wider bandgap. Also, increasing R can deteriorate the attenuation strength as the value of the transmission ratio is increased from $R = 5\Omega$ to $R = 10\Omega$ under same δ value, i.e., the appropriate R value selection is necessary to smooth the curve and avoid worse attenuation strength at the same time.

Comparing smoothed transmission ratio curves, the lowest value of transmission ratio with NC integration (0.1 for $\delta = -1.1$, $R = 5\Omega$) is much smaller than that of the graded beam without NC integration (0.53 for $\delta = 0$, $R = 10\Omega$), resulting in an 81% reduction of transmission ratio. This means that the NC enhances the wave attenuation strength of current graded piezoelectric metamaterial beam, which paves a path for addressing the pseudo bandgap issue of current graded piezoelectric metamaterial beam.

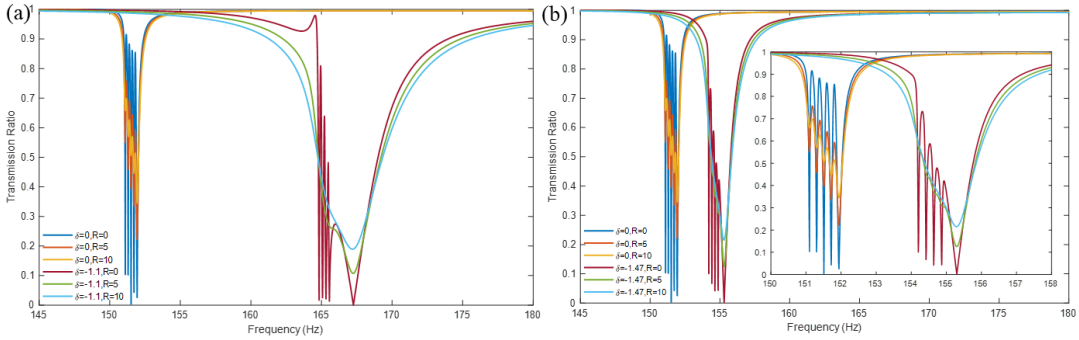

Figure 4. Transmission ratio responses of non-uniform metamaterials with different load resistance ($R = 0$, $R = 5$, $R = 10$) under: (a) $\delta = -1.1$, (b) $\delta = -1.47$

The effect of NC integration on frequency spacing Δf of graded piezoelectric metamaterial beam is analyzed in Figure 5. As mentioned, the frequency spacing Δf has a decisive influence on the graded beam without NC integration, i.e., the increasing Δf leads to unsuccessful aggregated gap due to the completely separate local resonant frequencies, while the smoothed curve exhibits even worse attenuation strength. In contrast, the proposed graded piezoelectric metamaterial beam with NC integration becomes much less sensitive to Δf, i.e., with NC integration, there is little difference between the dash-dotted transmission ratio curves with $\Delta f = -0.2Hz$ and $\Delta f = -0.5Hz$ in Figure 5. When the frequency spacing becomes large ($\Delta f = -1Hz$), the NC integration can "aggregate" the complete separated resonant peaks to continuous bandgap. This mitigated frequency spacing sensitivity effect of NC integrated graded piezoelectric metamaterial beam can provide potential solutions to overcome the frequency overlapping limitations.

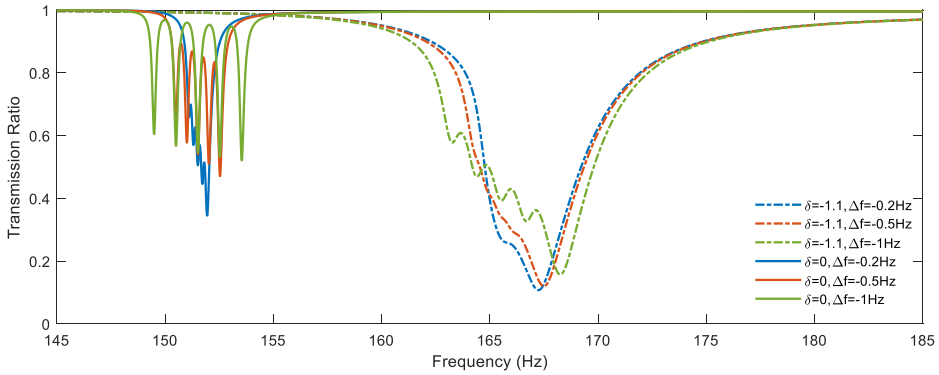

Figure 5. Transmission ratio responses of non-uniform metamaterials with different Δf and δ for $R = 5$.

5. CONCLUSION

This research presents a graded piezoelectric metamaterial beam with non-uniform LC shunts integrated with negative capacitance (NC) element. The grading is formed by non-uniform inductance in local resonant shunt circuits, keeping the resistance fixed for smoothing effect. Identical NC is connected in series to the graded LC resonant shunt circuit for performance enhancement. Based on the transmission ratio values computed using the transformation matrix method, it is identified that the NC integration not only enables further broadening of the aggregated bandgap, but also improves the attenuation strength as compared to the conventional graded piezoelectric metamaterial beam. In terms of system requirements, the NC integrated non-uniform configuration requires smaller inductance for practical implementation and smaller load resistance for smoothing effect. Additionally, the attenuation strength after smoothing is also improved by the introduction of NC elements.

ACKNOWLEDGMENTS

This research was supported in part by NSF under grant CMMI – 1825324.

REFERENCES

[1] H. Danawe, G. Okudan, D. Ozevin, S. Tol, "Conformal gradient-index phononic crystal lens for ultrasonic wave focusing in pipe-like structures," *Applied Physics Letters*, vol. 117, no.2, Jul. 2020.

[2] G. Trainiti, Y. Xia, J. Marconi, G. Cazzulani, A. Erturk, M. Ruzzene, "Time-periodic stiffness modulation in elastic metamaterials for selective wave filtering Theory and experiment," *Physical review letters*, vol.122, no.12, Mar. 2019.

[3] Y. Li, E. Baker, T. Reissman, C. Sun, WK. Liu, "Design of mechanical metamaterials for simultaneous vibration isolation and energy harvesting," *Applied Physics Letters*, vol. 111, no. 25, Dec. 2017.

[4] G. Ji, J. Huber, "Recent progress in acoustic metamaterials and active piezoelectric acoustic metamaterials-A review," *Applied Materials Today*. Vol. 27, Nov. 2021.

[5] JM. Dupont, T. Wang, J. Tang, "Phase-shift analysis of locally resonant piezoelectric metasurface," *In Health Monitoring of Structural and Biological Systems XVI*, Vol. 12048, pp. 163-169. SPIE. 2022.
[6] H. Fang, SC. Chu, Y. Xia, KW Wang, "Programmable self-locking origami mechanical metamaterials," *Advanced Materials*, vol. 30, no. 15, Apr. 2018.
[7] Z. Lu, X. Yu, SK. Lau, BC. Khoo, F. Cui, "Membrane-type acoustic metamaterial with eccentric masses for broadband sound isolation," *Applied Acoustics*, vol. 157, Jan. 2020.
[8] GL. Huang, CT. Sun, "Band gaps in a multiresonator acoustic metamaterial," *Journal of Vibration and Acoustics*. Vol. 132, no. 3, Jun. 2010.
[9] W. Zhou, W. Chen, Z. Chen, C. Lim, "Actively controllable flexural wave band gaps in beam-type acoustic metamaterials with shunted piezoelectric patches," *European Journal of Mechanics-A/Solids*, vol. 77, Sep. 2019.
[10] X. Xiao, ZC He, E. Li, B. Zhou, XK. Li, "A lightweight adaptive hybrid laminate metamaterial with higher design freedom for wave attenuation," *Composite Structures*, vol. 243, Jul. 2020.
[11] Y. Xia, M. Ruzzene, A. Erturk, "Dramatic bandwidth enhancement in nonlinear metastructures via bistable attachments," *Applied Physics Letters*, vol. 114, no. 9, Mar. 2019.
[12] B. Bao, M. Lallart, D. Guyomar, "Manipulating elastic waves through piezoelectric metamaterial with nonlinear electrical switched Dual-connected topologies," *International Journal of Mechanical Sciences*, vol. 172, Apr. 2020.
[13] Y. Jian, L. Tang, G. Hu, Z. Li, KC. Aw, "Design of graded piezoelectric metamaterial beam with spatial variation of electrodes," *International Journal of Mechanical Sciences*, vol. 218, Mar. 2022.
[14] G. Hu, AC. Austin, V. Sorokin, L. Tang, "Metamaterial beam with graded local resonators for broadband vibration suppression," *Mechanical Systems and Signal Processing*, vol. 146, Jan. 2021.
[15] M. Alshaqaq, A. Erturk, "Graded multifunctional piezoelectric metastructures for wideband vibration attenuation and energy harvesting," *Smart Materials and Structures*, vol. 30, no. 1, Dec. 2020.
[16] YY. Chen, R. Zhu, MV. Barnhart, GL. Huang, "Enhanced flexural wave sensing by adaptive gradient-index metamaterials," *Scientific reports*. Vol. 6, no. 1, Oct. 2016.
[17] Y. Jian, L. Tang, G. Hu, Y. Wang, KC. Aw. "Adaptive genetic algorithm enabled tailoring of piezoelectric metamaterials for optimal vibration attenuation," *Smart Materials and Structures*, vol. 31, no. 7, Jun. 2022.
[18] Y. Liu, C. Han, D. Liu, "Broadband vibration suppression of graded/disorder piezoelectric metamaterials," *Mechanics of Advanced Materials and Structures*. Vol. 6, Jan. 2022.
[19] T. Wang, J. Dupont, J. Tang, "Enhanced passive vibration suppression using self-powered piezoelectric circuitry integration," *In Active and Passive Smart Structures and Integrated Systems XVI*, Vol. 1204, SPIE. 2022.
[20] T. Wang, J. Tang, "Parametric Analysis of Negative Capacitance Circuit for Enhanced Vibration Suppression Through Piezoelectric Shunt," *In International Design Engineering Technical Conferences and Computers and Information in Engineering Conference*, vol. 86311, ASME. 2022.